EPJ Web of Conferences **302**, 06001 (2024) https://doi.org/10.1051/epjconf/202430206001
SNA + MC 2024

Thermal behavior analysis of monolayer and bulk UAl_3 at room temperature

Eui-Hyun Kong[1*], *Byoungjin So*[2], and *Young-Wook Tahk*[1]

[1]KAERI, Multi-purpose Small Reactor Fuel Development Division, 34022 Daejeon, Republic of Korea
[2]KAERI, Advanced Fuel Cycle Technology Division, 34022 Daejeon, Republic of Korea

Abstract. UAl_3 has been widely used as a target material for the production of ^{99}Mo. To safely produce radioactive isotopes from UAl_3, it is crucial to understand and predict the thermal behavior of UAl_3. Directly measuring the thermal properties of UAl_3 due to the radiation generated in nuclear fuel material is challenging. As an alternative, using the molecular dynamics (MD) simulator LAMMPS, the thermal conductivities of monolayer and bulk UAl_3 are predicted. In this study, it is primarily observed that the absence of the third-order anharmonic constant along the z-axis contributes to a higher thermal conductivity of monolayer UAl_3 compared to bulk UAl_3. Furthermore, the calculated thermal conductivity of bulk UAl_3 falls within the range of the measured values in the literature.

1 Introduction

^{99}Mo, formed through the nuclear fission of low-enriched uranium with ^{235}U content of less than 20 wt.%, is a parent isotope of ^{99m}Tc, widely utilized in medical imaging diagnostics. ^{99m}Tc is known for its short half-time (half-life: 6 hours) and low radiation energy, resulting in low internal radiation exposure. Its excellent tissue penetration properties contribute to high diagnostic accuracy. ^{99m}Tc can be synthesized in the form of labeled compounds that accumulate in most organs of the body, making it widely utilized in various diagnoses [1].
Currently, South Korea relies partially on imports for medical and industrial isotopes. To promote domestic self-sufficiency and facilitate international exports of the isotopes dependent on imports, 15 MWt open-tank-in-pool type Kijang research reactor (KJRR) is under construction. The target material to be used for ^{99}Mo production in KJRR consists of a meat with spherical uranium aluminide (UAl_x) particles dispersed in a pure aluminium matrix, surrounded by a cladding material made of aluminium alloy [2]. The uranium density of the meat is 2.6 g-U/cm^3 and the uranium enrichment is 19.75 wt.% ^{235}U. UAl_x is predominantly composed of UAl_3, with the remainder being UAl_4. The target material is scheduled for neutron irradiation over a period of 7 days in KJRR, with an expected burnup of less than 5% ^{235}U.

* Corresponding author: euihyun@kaeri.re.kr

© The Authors, published by EDP Sciences. This is an open access article distributed under the terms of the Creative Commons Attribution License 4.0 (https://creativecommons.org/licenses/by/4.0/).

2 Theoretical method

The crystal structure of UAl_3 belongs to the cubic space group $Pm\bar{3}m$, as illustrated in Fig. 1, with a lattice constant of 4.26 Å. The MD simulator used for the thermal behavior analysis of UAl_3 is LAMMPS (large-scale atomic/molecular massively parallel simulator) [3]. LAMMPS, developed collaboratively by Sandia national laboratory and Lawrence Livermore national laboratory, is an open-source, parallelized molecular dynamics package capable of solving large-scale problems. It supports parallel processing using MPI (message passing interface).

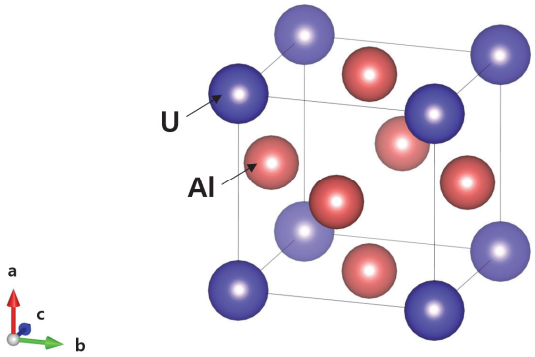

Fig. 1. Crystal structure of UAl_3

The MD simulates the motion of molecules by calculating the forces between them, exploring the properties of materials. In other words, it iteratively calculates Newton's equations of motion for particles at the current time (t) to determine the positions, velocities, forces, and other attributes of particles at the next time (t+Δt), ultimately computing various physical properties. In MD, the most computationally demanding aspect is typically the calculation of forces between each pair of particles, which is done using a potential function.
The interatomic potential energy used in this study is defined using the many-body potential, MEAM (modified embedded-atom method) potential [4]. In the MEAM, the total energy of a system is approximated as:

$$E = \sum_i \left[F_i(\bar{\rho}_i) + \frac{1}{2} \sum_{i \neq j} \phi_{ij}(r_{ij}) \right]$$

$F_i(\bar{\rho}_i)$ presents the embedding energy, indicating the energy change when an impurity atom occupies the site of i-atom with the background electron density of $\bar{\rho}_i$. As $\bar{\rho}_i$is determined by s, p, d, and f atomic electron densities, the term $F_i(\bar{\rho}_i)$ reflects the many-body effects. The term $\phi_{ij}(r_{ij})$ represents the pair potential when atoms i and j are separated by a distance r_{ij}. Table 1 lists the potential parameters for the Al-U [5] used in this study.

Table 1. Potential parameters of Al-U

Potential parameter	Value
α	5.5364807
E_c	4.0435039
$r_e(\text{Å})$	3.0432685
$\bar{\rho}^0{}_{U/Al}$	2.2488211
$C_{min}(112)$	1.2094229
$C_{min}(121)$	0.2558103
$C_{min}(122)$	0.2019148
$C_{min}(221)$	0.4418066
$C_{max}(112)$	1.4792962
$C_{max}(121)$	2.0880558
$C_{max}(122)$	1.9424523
$C_{max}(221)$	1.0510265

α : $\alpha = (9\text{B}\Omega E_c)^{1/2}$, B is the bulk modulus and Ω is the equilibrium atomic volume
E_c : cohesive energy
r_e : equilibrium nearest-neighbor distance
$\bar{\rho}^0_{U/Al}$: background electron density for Al-U alloy
C_{min}, C_{max} : account for many-body screening effects

2.1 System minimization

For system stabilization, the Polak-Ribière version of the conjugate gradient method, known for faster convergence than gradient descent, was utilized. The time-integration algorithm employed the Velocity-Verlet method, which offers lower errors and simpler programming compared to the Euler method. Initial velocities of atoms were assigned using Gaussian random numbers. The ensemble methods NVE (microcanonical ensemble) and NPT (isothermal-isobaric ensemble) were applied.
The periodic boundary conditions for both the monolayer and bulk UAl_3 are set as 2347×7×1 and 2347×7×5 which contain 65,716 and 328,580 atoms, respectively.
Figure 2 depicts the changes in temperature, pressure, and volume of the system, as well as the kinetic energy and potential energy of particles during the relaxation process. It is observed that each of these values generally stabilize after simulation time of approximately 400 ps.

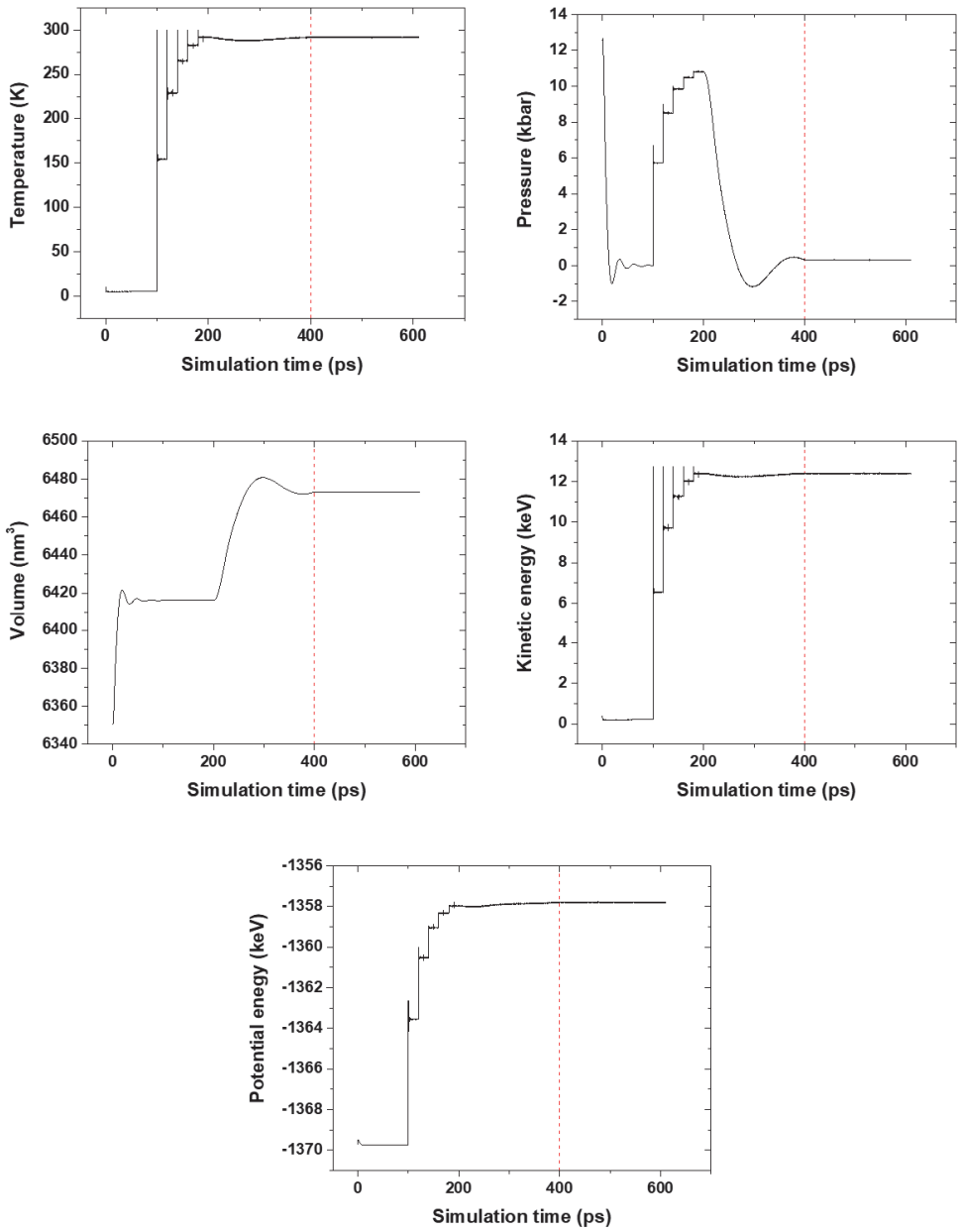

Fig. 2. System relaxation process of UAl_3 (2347×7×5)

2.2 Calculation of thermal conductivity

The thermal conductivity evaluation method employed non-equilibrium molecular dynamics using direct methods [6] similar to experimental measurements. Applying heat at the 1/4 position and removing heat at the 3/4 position along the x-axis of the system, as depicted in Fig. 3, yields the heat flux (J_x) by equation (1) when the system reaches equilibrium. Consequently, the temperature gradient (dt/dx) of the system is calculated, and ultimately, the thermal conductivity (k_x) is obtained through Fourier's law in equation (2).

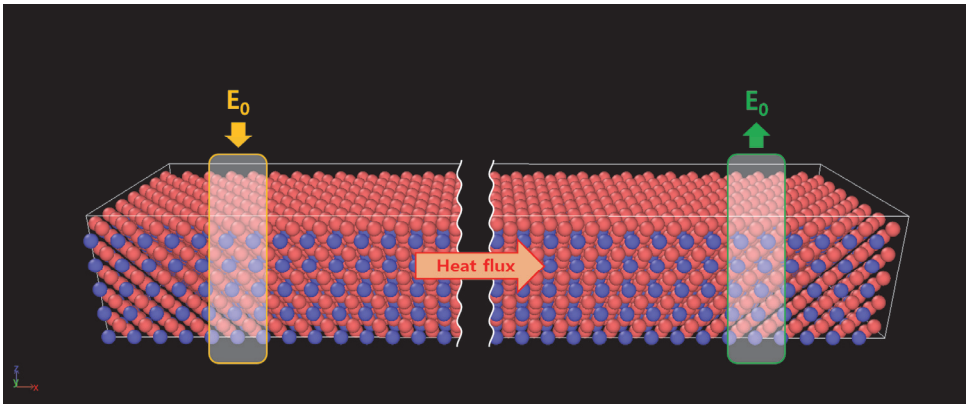

Fig. 3. Schematic of the simulation system to calculate thermal conductivity of UAl_3

$$J_x = -\frac{1}{2}\frac{E_0}{A \times \Delta t} \tag{1}$$

E_0 represents the heat added to or removed from the system, Δt is the time interval during which the heat is applied, and A is the cross-sectional area of the system.

$$J_x = -k_x \frac{dT}{dx} \tag{2}$$

The timestep in this study is 1 fs. The example of the temperature profile for UAl_3 is shown in Fig. 4. It is observed that the system reaches a steady state at a simulation time of approximately 12 ns in Fig. 4(a).

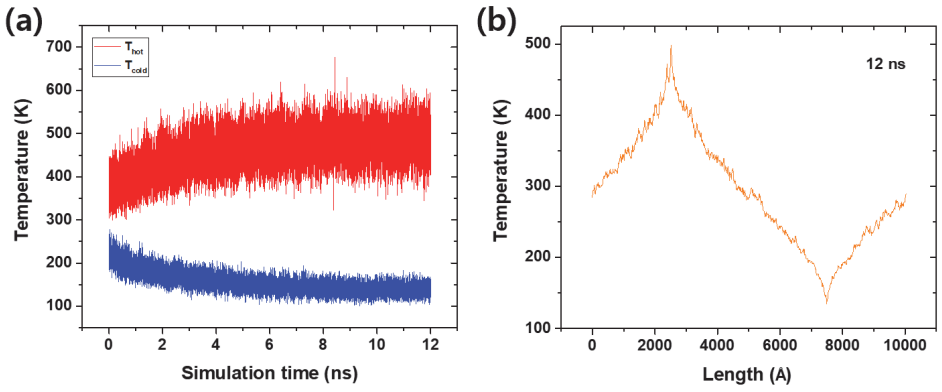

Fig. 4. Temperature profiles of UAl_3 (2347×7×1)

2.3 Phonon analysis

For the analysis of thermal behaviour, phonon dispersion was calculated using 'Phonon' [7] fix provided by LAMMPS. The 'Phonon' fix receives the temporary positions of atoms in an equilibrium system, transforms it into reciprocal space to obtain the Green's function coefficients. After a specific measurement, the time average of Green's function coefficients is evaluated, and over a sufficiently long simulation, it can resemble an ensemble average. The force constant matrix is created based on the generated dynamical matrix. The results are recorded in log files and binary files. The binary files utilize the 'Phana' code for phonon frequency calculations. After reaching equilibrium, the 'Phana' code produces phonon dispersion curves.

3 Results and Discussion

The thermal conductivities at room temperature for monolayer and bulk UAl_3 calculated from time-averaged temperature profiles such as Fig. 4(b) are ~20.0 W/m-K and ~9.4 W/m-K, respectively.

The higher thermal conductivity of the monolayer than the bulk can be attributed to the faster phonon group velocity of the monolayer compared to the bulk, as observed in other materials [8]. However, the acoustic phonon group velocities along the (1/2,0,0) calculated from Figs. 5(b) and 5(c), indicate a nearly indistinguishable similarity between monolayer UAl_3 and bulk UAl_3.

In the case of the monolayer, the absence of the third-order anharmonic constant along the z-axis has been reported to lead to a lower phonon scattering rate (inverse of phonon lifetime) calculated using the third-order anharmonic constant [8], contributing to explaining the higher thermal conductivity of the monolayer compared to the bulk. In Figs. 5(d) and 5(e), it is confirmed that due to the absence of the third-order anharmonic constant along the z-axis, the phonon group velocity along the R−M path of the phonon dispersion curve for monolayer UAl_3 becomes zero, unlike bulk UAl_3.

The thermal conductivity of UAl_3 calculated by MD simulations in this study was found to be lower than the values computed using ab initio molecular dynamics (AIMD) calculations in the literature [9]. In the phonon dispersion relations for bulk UAl_3 calculated using AIMD calculation in Fig. 6, the acoustic phonon modes influencing thermal conduction are distinctly separated from the optical phonon modes. However, in the phonon dispersion relations obtained in this study, it is observed that acoustic and optical phonon modes overlap in Fig. 5. This overlap is considered one of the reasons explaining the lower thermal conductivity calculated by MD simulations.

In conclusion, the calculated thermal conductivity (~9.4 W/m-K) of the bulk UAl_3 falls within the measured range of 4.18 to 12.55 W/m-K in the literature [10]. When considering the absence of phonon-defect scattering and phonon-electron scattering, MD simulations in this study seem to effectively simulate the thermal behavior of the bulk UAl_3.

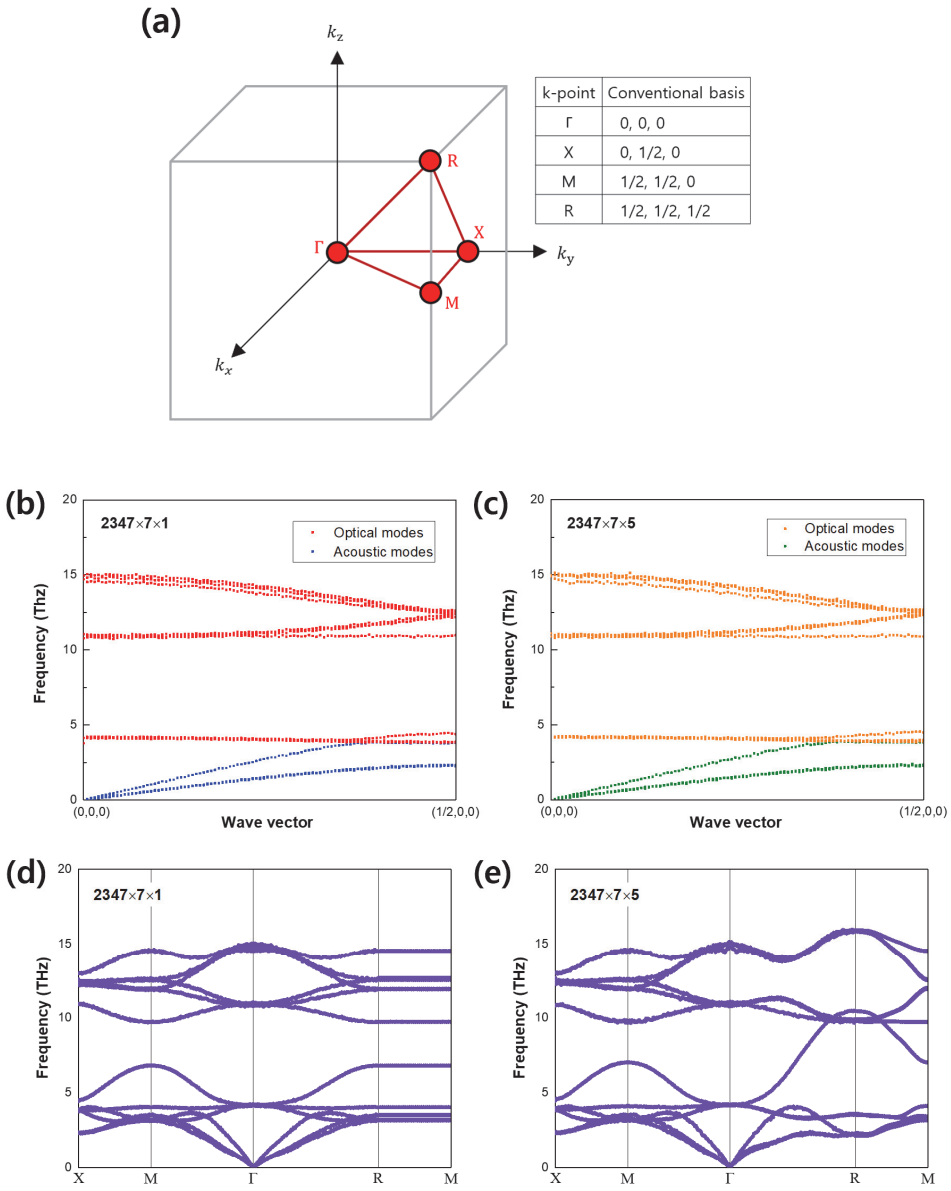

Fig. 5. Phonon dispersion relations of UAl_3 : (a) Brillouin zone of $Pm\bar{3}m$, (b,d) monolayer UAl_3, (c,e) bulk UAl_3

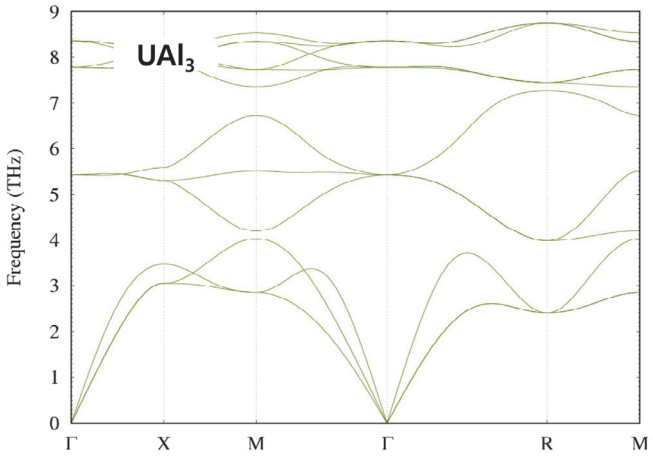

Fig. 6. Phonon dispersion relations of UAl_3 obtained using AIMD calculations at 300K [9]

This study was supported by the National Research Foundation of Korea (NRF) grant funded by the Korean government (MSIT: Ministry of Science and ICT) (NRF-2020M2C1A1061031).

References

1. Health Campus, https://humanhealth.iaea.org
2. H. J. Ryu, C. K. Kim, M. Sim, J. M. Park, J. H. Lee, Nucl. Eng. Technol., **45** 979 (2013)
3. LAMMPS Molecular Dynamics Simulator, https://lammps.org
4. B.-J. Lee, M. I. Baskes, Phys. Rev. B, **62** 8564 (2000)
5. M. I. Pascuet, J. R. Fernández, J. Nucl. Mater., **467** 229 (2015)
6. P. K. Schelling, S. R. Phillpot, P. Keblinski, Phys. Rev. B, **65** 144306 (2002)
7. L. T. Kong, Comput. Phys. Commun., **182** 2201 (2011)
8. X. Gu, B. Li, R. Yang, J. Appl. Phys., **119** 085106 (2016)
9. Z.-G. Mei, Y. S. Kim, A. M. Yacout, J. Yang, X. Li, Y. Cao, Materialia, **4** 449 (2018)
10. T. I. Jones, K. N. Street, J. A. Scoberg, J. Baird, Can. Metall. Quart., **2** 53 (1963)